

# APPLICATION OF AN ADAPTIVE STABLE GFEM FOR FRACTURE PROPAGATION IN PLAIN CONCRETE

Abdelrahman M. El-Tohfa<sup>1</sup> AND Faisal M. Mukhtar<sup>2,3</sup>

<sup>1</sup> Dept. of Civil and Env. Eng., King Fahd University of Petroleum & Minerals,  
Dhahran 31261, Saudi Arabia, g201474960@kfupm.edu.sa

<sup>2</sup> Dept. of Civil and Env. Eng., King Fahd University of Petroleum & Minerals,  
Dhahran 31261, Saudi Arabia, faisalmu@kfupm.edu.sa

<sup>3</sup> Interdisciplinary Research Center for Construction and Building Materials, King Fahd  
University of Petroleum & Minerals, Dhahran 31261, Saudi Arabia

**Key words:** 3-D concrete fracture propagation, Size effect, Generalized/eXtended finite element method, Bilinear cohesive model

**Abstract.** Generalized finite element method (GFEM) has proven itself as a tool of choice over the conventional FEM in fracture analysis due to enhanced computational efficiency as well as allowing cracks to propagate independently of the domain mesh – Thanks to the use of enrichments chosen based on the a priori knowledge of the solution behavior. With the many versions of the method’s formulations in the literature, their stability issues, compared to the standard FEM, are often unresolved. This paper presents the use of an adaptive stable GFEM to plain concrete fracture propagation. Having verified the formulation’s accuracy and stability based on the Linear Elastic Fracture Mechanics in previous studies and its two-scale (global-local) version on concrete fracture, the present work seeks to verify its capabilities in capturing the size effect behavior in concrete. A set of fracture simulations in geometrically similar experimental concrete beams, under a 3-point bending regime, is presented based on a bilinear cohesive model. In addition to the GFEM’s agreement with the experimental load-displacement response and the effect of the initial notch-to-depth ratio, the simulation successfully captures the size effect behavior when presented on the popular Type II Size Effect plot – the so-called Bazant’s law.

## 1 INTRODUCTION

Due to the large fracture process zone in concrete, the structural size effect, which inversely affects the nominal strength, is observed and renders the linear elastic fracture mechanics inapplicable. Thus, softening models – either energy-based that depends on the material characteristics or statistical-based based on reverse analysis – are used for simulating concrete fractures.

In terms of solution tools, various numerical methods have been applied to simulate concrete fracture, including the finite element method (FEM) [1], the boundary element method [2], and the lattice model [3], to mention a few. FEM has been the building block for developing other discretization methods. However, preparation of the domain mesh in FEM takes up to 80 % of the analysis time [4] as crack propagation is limited to interface elements. Unfortunately,

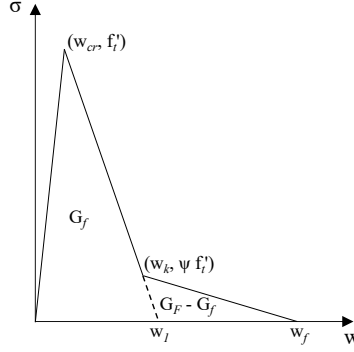


**Figure 1:** Concrete bilinear softening model

the limitation of crack surfaces to the elements' interface requires the utilization of re-meshing algorithms, thereby increasing the computational cost of the analysis. The generalized finite element method (GFEM) is a special finite element method based on the partition of unity. The enriched formulation in the GFEM allows cracks to propagate through domain elements, independent of the problem morphology, due to proper use of enrichment functions. Thus, GFEM mesh can be simple and structured contrary to that of the FEM, thereby improving computational efficiency. In addition to the use of discontinuity function, such as the Heaviside function, GFEM can utilize singular enrichments around the crack front if specific characteristics of the solution are known a priori, as is the case in concrete fracture. This improves solution convergence with minimum  $h$ -refinement.

This paper validates the ability of a GFEM to simulate crack propagation in concrete. An energy-based bilinear softening cohesive model is utilized to show the GFEM's capability to capture the size effect in concrete fracture. The paper starts with an overview of the GFEM presented in Section 2. Then, the 3D fracture of a set of geometrically similar concrete beams is simulated in Section 3, followed by verifying the GFEM results – against the experimental predictions – on Bazant's type II size effect plot [5]. Lastly, the GFEM's ability to capture the effect of the initial notch-to-depth ratio on concrete fracture is shown.

## 2 GENERALIZED FINITE ELEMENT METHOD OVERVIEW

The generalized finite element method (GFEM) is based on the partition of unity for enriching mesh-free approximation. The basic framework of the GFEM is that any function can be reproduced by a product of the partition of unity function with the function itself [6]. The method is an offshoot of thorough research in meshfree methods [7, 8]. Due to its independence of the problem morphology, the method is particularly advantageous in analyzing problems that possess discontinuities, localized deformation, singularity, and complex geometry characteristics. GFEM can utilize discontinuous and singular enrichments at the crack surface and front, respectively. Alternatively, it may only utilize discontinuous enrichments on the crack surface.

This study utilized the adaptive 3D GFEM whose accuracy and stability have been validated based on the Linear Elastic Fracture Mechanics by Sanchez-Rivadeneira and Duarte [9], and its global-local version for concrete fracture by Kim and Duarte [10]. Here, we validate the

method's ability to capture the size effect behavior based on the bilinear cohesive zone model (shown in Fig. 1) for concrete fracture by utilizing only discontinuous enrichments to simulate cohesive fracture propagation. The GFEM approximation was formulated as a summation of the traditional finite element approximation and an enrichment term as given by Eq. (1).

$$u^h(x) = \sum_{\alpha \in I_h} \hat{u}_{\alpha o} \varphi_{\alpha}(x) + \sum_{\alpha \in I_h^H} \varphi_{\alpha}(x) \sum_{j=0}^{\hat{m}_{\alpha}} \tilde{u}_{\alpha j} \hat{E}_{\alpha j}(x) \quad (1)$$

The first summation in Eq. (1) represents the finite element approximation for the bulk domain with  $\hat{u}_{\alpha o}$  as the degrees of freedom and  $\varphi_{\alpha}$  the FEM shape function. The second summation represent the GFEM approximation enriched with the function  $\hat{E}_{\alpha j}$ .  $\tilde{u}_{\alpha j}$  represents the degrees of freedom for the second term.  $I_h$  and  $I_h^H$  are the set of unenriched FEM nodes and the set of enriched nodes cut by the crack surface, respectively. The GFEM enrichment is, therefore, obtained as the product between the FEM shape  $\varphi_{\alpha}$  and the enrichment function  $\hat{E}_{\alpha j}$ , where the Heaviside function was used as the enrichment.

### 3 NUMERICAL SIMULATIONS

A set of geometrically similar concrete beams, on one hand, and equal-sized concrete beams of different notch-to-depth ratios, on the other hand, were used to illustrate the 3D GFEM capabilities in simulating concrete fracture and capturing the size effect using the bilinear softening model. The solutions were obtained based on a non-linear Newton-Raphson algorithm. Section 3 in Kim and Duarte [10] provides further details about the GFEM. Details about the softening cohesive law are available in section 2 of the same reference.

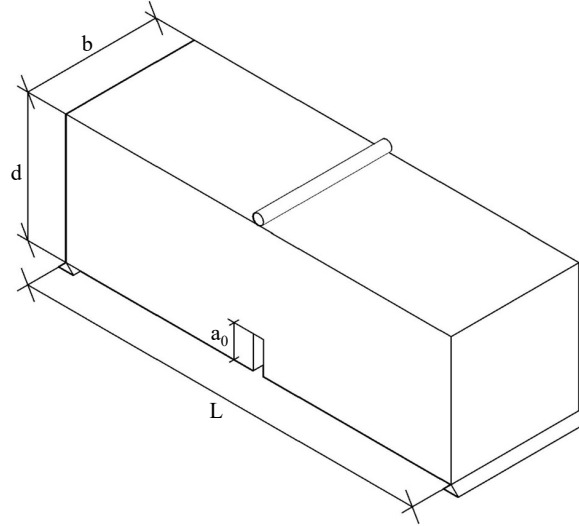


**Figure 2:** Beam configuration

The experiments of the concrete beams (selected here for the simulation) were carried out by Dong et al. [11]. The problem configuration is shown in Fig. 2 and the geometries and material

properties of two-beam groups (L and B) used in the simulation are described in Table 1. Group L represents the fracture of three geometrically similar beams tested under three-point bending. A span-to-depth ratio of 4.0 and an initial notch-to-depth ratio of 0.4 were adopted. Group B represents the fracture of four identical beams with different initial notch-to-depth ratios ranging from 0.2 to 0.6. The material properties of the two groups are different, with Group L having a higher initial fracture toughness ( $G_f$ ) than that of Group B, which plays a role in affecting their fracture responses.

**Table 1:** Dimension and material properties of simulated beams

Beam	L x d x b mm x mm x mm	$a_0$ mm	$G_f$ N/mm	$G_F$ N/mm	CTOD <sub>c</sub> mm	E GPa	$\nu$	$f'_t$ MPa
L1	400 x 100 x 100	40	0.097	0.11	0.0717	24	0.2	2.3
L2	800 x 200 x 100	80	0.153	0.17	0.1131	24	0.2	2.3
L3	1200 x 300 x 100	120	0.141	0.16	0.1042	24	0.2	2.3
B2	600 x 150 x 40	30	0.096	0.11	0.0680	28	0.2	2.4
B3	600 x 150 x 40	45	0.098	0.11	0.0694	28	0.2	2.4
B4	600 x 150 x 40	60	0.0925	0.10	0.0655	28	0.2	2.4
B6	600 x 150 x 40	90	0.108	0.12	0.0765	28	0.2	2.4

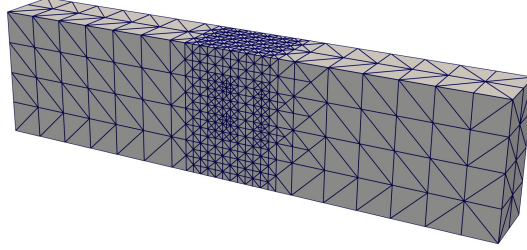


**Figure 3:** Typical GFEM domain mesh

The elastic modulus ( $E$ ), Poisson ratio ( $\nu$ ), tensile strength ( $f'_t$ ), and initial fracture toughness ( $G_f$ ) are taken directly from Dong et al. [11]. The ratio between the total fracture toughness ( $G_F$ ) and the initial fracture toughness ( $G_f$ ) was calibrated and kept constant for all the beams to better match the experimental post-peak response in line with Hoover and Bažant [12]. However, unlike in Hoover and Bažant [12], the critical crack-tip-opening displacement (CTOD<sub>c</sub>) was not calibrated. Instead, we calculated it based on Eq. (2) [13].

$$\psi = 1 - \frac{\text{CTOD}_C f'_t}{2G_f} = 0.15 \quad (2)$$

Tetrahedral elements of size equal to one-fourth of the beam depth were used in all the GFEM simulations. Using a bisection algorithm, elements within 50 mm of the beam midspan were refined four times for the 100 mm and 150 mm deep beams, and six times for the 200 mm and 400 mm deep beams. Fig. 3 shows a typical example of such a mesh generated for the simulation.

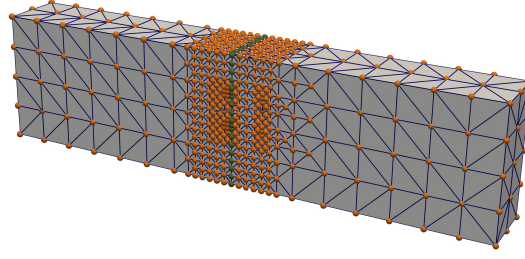


**Figure 4:** GFEM enrichment. Green and orange spheres represent Heaviside enriched nodes and unenriched nodes, respectively

Fig. 4 shows the enrichment distribution in the GFEM mesh, with green spheres representing the Heaviside enriched nodes, while the unenriched nodes are represented by orange spheres.

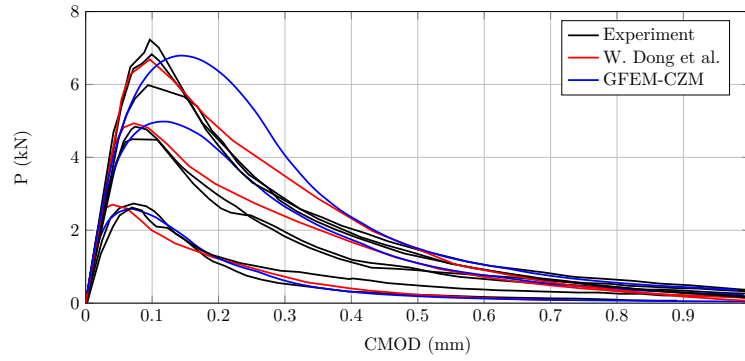


**Figure 5:** Load versus CMOD for the fracture of L beam series

Plots of the load versus crack mouth opening displacement (CMOD) comparing the experimental results with the numerical predictions by the GFEM for the geometrically similar concrete beams (L1, L2, and L3) are shown in Fig. 5. The figure shows evidence of the GFEM's ability to successfully predict the peak load. Possibly, due to the high initial fracture toughness reported in the experiment, the GFEM overestimated the beginning of the post-peak softening response of L2 and L3. On the other hand, for beams with lower initial fracture toughness, such as L1 and the B group, the GFEM successfully predicted the softening post-peak behavior, as seen in the L1 results in Fig. 5 and, as it will be seen later, for the B group.

Size effect laws are models used to describe the concrete size effect caused by the presence of a fracture process zone. Bažant's type II size effect law [5] applies to notched concrete structures. Given by Eq. (3), the law describes the concrete nominal stress  $\sigma_N$  in terms of the tensile strength  $f'_t$  and the empirical constants  $B$  and  $d_0$  which are determined using the linear regression analysis based on Eq. (4).

$$\sigma_N = \frac{B f'_t}{\sqrt{1 + \frac{d}{d_0}}} \quad (3)$$

$$Y = AX + C \quad (4)$$

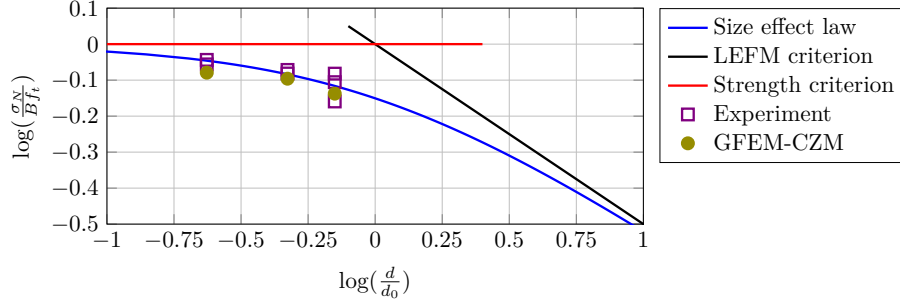


**Figure 6:** Type II size-effect plot for the L beam series

where,

$$Y = \left(\frac{1}{\sigma_N}\right)^2, \quad X = d, \quad Bf'_t = \frac{1}{\sqrt{C}}$$

Experimental and GFEM numerical results for the L beam series are presented on the Type II size effect plot in Fig. 6 based on the regression analysis that resulted in  $A = 0.0244 \text{ mm}^{-1}$ ,  $C = 10.35 \text{ MPa}^{-2}$ ,  $d_0 = 424.42 \text{ mm}$ , and  $Bf'_t = 0.3107 \text{ MPa}$ . This figure illustrates the GFEM's ability to capture the size effect behavior successfully. For the B beam series, where the effect of the initial notch-to-depth ratio was meant to be studied, Fig. 7 shows the load-CMOD behavior predicted by the GFEM compared to the experiments. The figure shows the success of the GFEM in predicting all the B specimens' peak loads and softening responses.

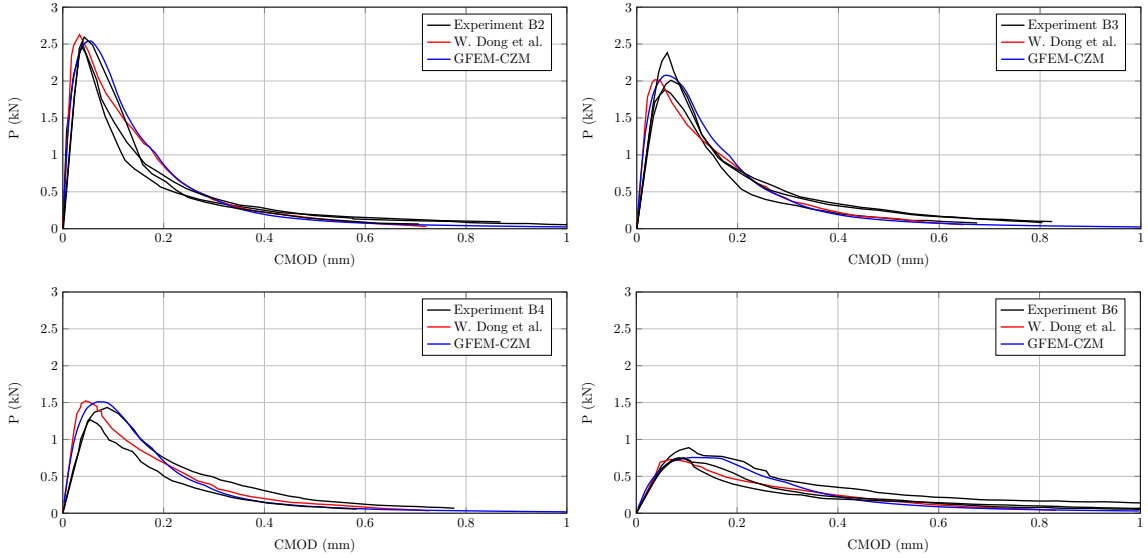


**Figure 7:** Load versus CMOD for fracture of B beam series

## 4 CONCLUSIONS

The generalized finite element method utilization of Heaviside enrichment allows for better computational efficiency in the simulation of problems with strong discontinuities, as is the case for concrete fracture. This enriched formulation allows fractures to propagate independently of the problem mesh morphology. The paper has presented the GFEM's capabilities for accurate prediction of the load versus CMOD behavior, the concrete size effect in geometrically similar beams, and the effect of notch-to-depth ratios on concrete fracture.

## 5 ACKNOWLEDGEMENTS

The authors acknowledge the financial support provided by the Deanship of Research Oversight and Coordination at King Fahd University of Petroleum & Minerals under Research Grant SB191024. F. M. Mukhtar specially thanks the Department of Civil & Environmental Engineering, University of Illinois at Urbana-Champaign for hospitality during his Visiting Scholar stay with Prof. C. A. Duarte Research Group in August, 2019.

## REFERENCES

- [1] Ingraffea, A. R., & Saouma, V. Numerical modeling of discrete crack propagation in reinforced and plain concrete. *Fracture mechanics of concrete: Structural application and numerical calculation* (1985) 171–225.
- [2] Saleh, A. L., & Aliabadi, M. H. Crack growth analysis in concrete using boundary element method. *Engineering fracture mechanics* (1995) **51**:533–545.
- [3] Chang, Z., Zhang, H., Schlangen, E., & Šavija, B. Lattice fracture model for concrete fracture revisited: Calibration and validation. *Applied Sciences* (2020) **10**:4822.
- [4] Cottrell, J. A., Hughes, T. J., & Bazilevs, Y. Isogeometric Analysis: Toward Integration of CAD and FEA. *John Wiley & Sons* (2009).
- [5] Bažant, Z. P. Size effect in blunt fracture: concrete, rock, metal. *Journal of engineering mechanics* (1984) **110**: 518-535.
- [6] C. Duarte, A. Simone, & A. Enriched Finite Element Methods: Theory and Practice. (2018). In preparation.
- [7] Moës, N., Dolbow, J., & Belytschko, T. A finite element method for crack growth without remeshing. *International Journal for Numerical Methods in Engineering* (1999) **46**:131–150.
- [8] Duarte, C. A., & Oden, J. T. An hp adaptive method using clouds. *Computer methods in applied mechanics and engineering* (1996) **139**:237–262.
- [9] Sanchez-Rivadeneira, A. G., & Duarte, C. A stable generalized/extended FEM with discontinuous interpolants for fracture mechanics. *Computer Methods in Applied Mechanics and Engineering* (2019) **345**:876-918.

- [10] Kim, J., & Duarte, C. A new generalized finite element method for two-scale simulations of propagating cohesive fractures in 3-D. *International Journal for Numerical Methods in Engineering* (2015) **104**:1139-1172.
- [11] Dong, W., Wu, Z., & Zhou, X. Calculating crack extension resistance of concrete based on a new crack propagation criterion.
- [12] Hoover, C. G., & Bažant, Z. P. Cohesive crack, size effect, crack band and work-of-fracture models compared to comprehensive concrete fracture tests. *International Journal of Fracture* (2014) **187**:133-143.
- [13] Park, K., Paulino, G. H., & Roesler, J. R. Determination of the kink point in the bilinear softening model for concrete. *Engineering Fracture Mechanics* (2008) **75**:3806-3818.